Lipid signaling via Pkh1/2 regulates fungal CO_2 sensing through the kinase Sch9

RUNNING TITLE: Sch9 regulates fungal CO_2 sensing

AUTHORS: Susann Pohlers[1], Ronny Martin[1,2], Thomas Krüger[3], Daniela Hellwig[1], Frank Hänel[4], Olaf Kniemeyer[2,3], Hans Peter Saluz[2,4], Patrick Van Dijck[5,6], Joachim F. Ernst[7], Axel Brakhage[2,3], Fritz A. Mühlschlegel[8,9] and Oliver Kurzai[1, 10, *]

AFFILIATIONS:

1) Septomics Research Center, Leibniz Institute for Natural Product Research and Infection Biology - Hans Knöll Institute (HKI), 07745 Jena, Germany
2) Friedrich Schiller University Jena, 07743 Jena, Germany
3) Department of Molecular and Applied Microbiology, Leibniz Institute for Natural Product Research and Infection Biology - Hans Knöll Institute (HKI), 07745 Jena, Germany
4) Department of Cell and Molecular Biology, Leibniz Institute for Natural Product Research and Infection Biology - Hans Knöll Institute (HKI), 07745 Jena, Germany
5) VIB Department of Molecular Microbiology, KU Leuven, 3000 Leuven, Belgium
6) Laboratory of Molecular Cell Biology, KU Leuven, 3000 Leuven, Belgium
7) Department Biologie, Molekulare Mykologie, Heinrich-Heine-Universität, 40225 Düsseldorf, Germany
8) Kent Fungal Group, School of Biosciences, University of Kent, Canterbury CT2 7NZ, UK
9) Clinical Microbiology Service, East Kent Hospitals University NHS Foundation Trust, The William Harvey Hospital, Ashford TN24 0LZ, UK
10) Center for Sepsis Control and Care, University Hospital Jena, 07743 Jena, Germany

***Correspondent footnote**

Oliver Kurzai, M.D.
Septomics Research Centre
Friedrich-Schiller-University Jena and
Leibniz-Institute for Natural Product
Research and Infection Biology – Hans Knöll - Institute
Albert-Einstein-Str. 10
07745 Jena
oliver.kurzai@leibniz-hki.de

Abstract

Adaptation to alternating CO_2 concentrations is crucial for all organisms. Carbonic anhydrases – metalloenzymes that have been found in all domains of life - enable fixation of scarce CO_2 by accelerating its conversion to bicarbonate and ensure maintenance of cellular metabolism. In fungi and other eukaryotes, the carbonic anhydrase Nce103 has been shown to be essential for growth in air (~0.04% CO_2). Expression of *NCE103* is regulated in response to CO_2-availability. In *Saccharomyces cerevisiae, NCE103* is activated by the transcription factor ScCst6, in *Candida albicans* and *Candida glabrata* by its homologue Ca/CgRca1. To identify the kinase controlling Cst6/Rca1, we screened a *S. cerevisiae* kinase/phosphatase mutant library for the ability to regulate *NCE103* in a CO_2-dependent manner. We identified ScSch9 as potential ScCst6-specific kinase, as the *sch9*Δ mutant strain showed deregulated *NCE103* expression on RNA and protein level. Immunoprecipitation revealed binding capability of both proteins and detection of ScCst6 phosphorylation by ScSch9 *in vitro* confirmed Sch9 as the Cst6 kinase. We could show that CO_2-dependent activation of Sch9, which is part of a kinase cascade, is mediated by lipid / Pkh1/2 signaling but not TORC1. Finally, we tested conservation of the identified regulatory cascade in the pathogenic yeast species *C. albicans* and *C. glabrata*. Deletion of *SCH9* homologues of both species impaired CO_2-dependent regulation of *NCE103* expression, which indicates a conservation of CO_2 adaptation mechanism among yeasts. Thus, Sch9 is a Cst6/Rca1 kinase that links CO_2 adaptation to lipid signaling via Pkh1/2 in fungi.

Importance [149 words]

All living organisms have to cope with alternating CO_2 concentrations as CO_2 levels range from very low in the atmosphere (0.04%) to high (5% and more) in other niches, including the human body. In fungi, CO_2 is sensed via two pathways. The first regulates virulence in pathogenic yeast by direct activation of adenylyl cyclase. The second pathway, although playing a fundamental role in fungal metabolism, is much less understood. Here the transcription factor Cst6/Rca1 controls carbon homeostasis by regulating carbonic anhydrase expression. Upstream signaling in this pathway remains elusive. We identify Sch9 as the kinase controlling Cst6/Rca1 activity in yeast and demonstrate that this pathway is conserved in pathogenic yeast species, which highlights identified key players as potential pharmacological targets. Furthermore, we provide a direct link between adaptation to changing CO_2 conditions and lipid / Pkh1/2 signaling in yeast, thus establishing a new signaling cascade central to metabolic adaptation.

Keywords

Carbon dioxide adaptation / carbon metabolism / *Saccharomyces cerevisiae* / CO_2 signaling / Candida

Introduction

Carbon dioxide is key to life on earth. Besides being RUBISCO's substrate in the carbon fixing component of the Calvin cycle it is the final product of cellular respiration (1). Consequently CO_2 plays a decisive role as a signaling molecule and its levels are sensed by organisms as diverse as bacteria, plants, fungi, nematodes, insects, fish and mammals (2, 3). In fungi, CO_2 impacts on fundamental biological characteristics including growth, morphology and virulence (4). For pathogenic fungi the ability to adapt to changing CO_2 is particularly relevant. When surviving as commensals on skin, fungi are exposed to atmospheric low CO_2 concentration, but when they invade their host, CO_2 concentrations can raise to 150-fold higher levels (5% or more) (5-7).

In fungi CO_2 is sensed via two distinct signaling pathways. In the first HCO_3^-, which is in equilibrium with membrane permeable CO_2 via action of the catalytic enzyme carbonic anhydrase (CA), directly activates adenylyl cyclases to signal via downstream protein kinase A (PKA) (8). This pathway was shown to trigger the yeast to hyphae switch of *Candida albicans* and capsule biosynthesis of *Cryptococcus neoformans* representing well characterized virulence factors of these major human pathogens (9, 10).

The second pathway is independent of adenylyl cyclase and much less characterized. This pathway directly affects cellular CO_2 fixation, HCO_3^- homeostasis and thus central metabolism. One read-out of this pathway is regulation of expression of the β-class fungal carbonic anhydrase (CA) Nce103p in response to environmental CO_2 (11, 12). CA are ubiquitous zinc-containing metalloenzymes, which accelerate the CO_2 to HCO_3^- interconversion and thus impact on carboxylation reactions and pH homeostasis (13-15).

Notably yeast CA expression is strongly induced in CO_2-limiting atmospheric conditions and downregulated in elevated CO_2 (11). The overarching significance of this second CO_2 sensing pathway for fungal biology is emphasized by the fact that deletion of yeast CA abolishes growth in low CO_2 (16).

CO_2 dependent regulation of CA is conserved in *Saccharomyces cerevisiae*, *Candida albicans* and *Candida glabrata*. Some insight into the signaling events mediating CO_2 dependent regulation of CA expression in yeast was recently gained by identifying the transcriptional activator regulator of carbonic anhydrase 1 (Rca1). Loss of Rca1 in the pathogenic yeasts *C. albicans* or *C. glabrata* and loss of the Rca1 orthologue Cst6 in *S. cerevisiae* led to a common phenotype, displaying lack of CA induction in low CO_2 (17, 18). Rca1/Cst6 belong to the ATF/CREB transcription factor family and have a C-terminal basic leucin zipper domain (19). Comparing the protein sequence of yeast Rca1/Cst6 revealed 3 conserved serine phosphorylation sites and loss of serine 124 in the *C. albicans* orthologue abolished CO_2-dependent regulation of downstream CA (17). This supports our hypothesis that Rca1/Cst6 phosphorylation is a critical step in yeast CO_2 sensing.

To unravel this novel CO_2 sensing pathway we used *S. cerevisiae* as model. Using high throughput kinase/phosphatase mutant library screening we identified Sch9 as the Cst6-specific kinase candidate. We confirmed direct interaction and phosphorylation of Cst6 by the Sch9 kinase and show that Cst6/Rca1 signaling is conserved in *C. albicans* and *C. glabrata* CO_2 sensing. Finally we provide evidence that Sch9 links CO_2-adaptation to lipid signaling via Pkh1/2.

Results

High throughput screening identifies potential Cst6 kinases

Previous work suggested that phosphorylation of the Cst6/Rca1 family of transcription factors is key to fungal CO_2 sensing, carbon fixation and metabolism (17). To test this hypothesis we opted for a high throughput approach to identify candidate kinases/phosphatases. CO_2 regulation in the model organism *S. cerevisiae* was previously reported to be particularly pronounced in response to CO_2 varying up to 20-fold between atmospheric and high CO_2 (11). Using qRT-PCR we confirmed this finding and found that CA mRNA levels are induced more than 23-fold when cultures are transferred from 5% CO_2 (*NCE103* ^{CO2}) to low CO_2 conditions (*NCE103* ^{air}), reaching maximum induction levels at 60 min (23.3 ± 4.9 fold induction, supplemental Fig. S1 A). Furthermore, we established that induction of *NCE103* ^{air} was reduced in *S. cerevisiae cst6*Δ (Fig. 1) and that *CST6* expression itself was not affected by CO_2 levels (supplemental Fig. S1 B). Since CA expression by CO_2 is conserved in these ascomycete yeasts, we decided to screen a *S. cerevisiae* kinase and phosphatase deletion mutant library of 155 strains (supplemental table S1) and quantify CO_2-dependent gene regulation (see supplemental table S2 for all data). Deletion of a Cst6 kinase should result in de-repression of CA in high CO_2 and consequently increased *NCE103* ^{CO2} expression at levels comparable to growth in air (supplemental Fig. S2) (17). Accordingly, mutants with mean *NCE103* ^{CO2} expression levels twice as high (≥ 2.0) as wild type (WT) were considered as putative kinase candidates. Of the 155 strains screened, 5 mutants met these criteria: *tpd3*Δ*, ptp1*Δ*, bud32*Δ*, sch9*Δ and *ptk2*Δ (Fig. 1, supplemental table S2 and S3). Among those, the *sch9*Δ mutant showed the highest upregulation of Sc*NCE103* ^{CO2} expression (3.55 ± 1.55), whereas Sc*NCE103* ^{air} expression (6.12 ± 2.98) was similar to WT. This

deregulation pattern resulted in a low fold change between Sc*NCE103* ^{air} and Sc*NCE103* ^{CO2} of 1.91 ± 0.7 (Fig. 1 and supplemental table S2). Furthermore, *sch9*Δ did not display general growth defects and *SCH9* encodes a kinase known to be involved in stress response via nutritional sensing in *S. cerevisiae* and adaptation to hypoxia in *C. albicans* (20-24), making Sch9 the most probable candidate as Cst6 kinase. To confirm our hypothesis we analyzed Nce103 protein level and fluorescence levels in a CA promotor – GFP fusion, then carried out immunoprecipitation experiments and finally showed that Sch9 phosphorylates Cst6.

Loss of Sch9 deregulates CO_2 sensing

Using a specific antibody against *S. cerevisiae* CA we measured protein levels in the *sch9*Δ mutant cultivated under different CO_2 conditions. In contrast to WT, Nce103 levels in *sch9*Δ were elevated regardless of the strain being exposed to low or high CO_2 (Fig. 2 A). Similar to *NCE103* gene expression, Nce103 protein level of *sch9*Δ was not strongly affected by environmental CO_2. Next we transformed WT, *cst6*Δ and *sch9*Δ cells with a plasmid containing GFP under control of the Sc*NCE103* promoter and exposed to low and high CO_2. GFP expression was analyzed using confocal microscopy (Fig. 2 B). GFP fluorescence of WT cells under 5% CO_2 was constantly very low, but fluorescence increased after incubation in air (6-fold after 60 min, 9-fold after 120 min, Fig. 2 B). The persistent increase over time is likely due to stability of GFP. In contrast, *cst6*Δ showed nearly undetectable fluorescence levels under both conditions. *sch9*Δ exhibited significantly higher fluorescence in 5% CO_2 compared to WT, but also higher intensity differences between cells. Fluorescence in air was comparable to WT. Noticeably, whereas *NCE103* expression levels of *cst6*Δ in air and *sch9*Δ in 5% CO_2 were not significantly different (Fig. 1), the GFP reporter signal

for *cst6*Δ in air was lower than for *sch9*Δ in high CO_2. This could be due to the intrinsically high variation of *NCE103* expression in air, which ranged from 3 to 10 when normalized to expression in 5% CO_2. Furthermore, the experimental setting differs, with the GFP reporter being expressed from a plasmid rather than from its native locus. However, results for *NCE103* levels in 5% CO_2 are consistent in both assays and confirm that loss of Sch9 leads to a loss of CO_2-dependent *NCE103* repression.

Sch9 is the Cst6 kinase

To demonstrate physical interaction between Cst6 and Sch9, immunoprecipitation experiments were performed. Endogenous ScCst6 was precipitated from WT lysate using a specific anti-Cst6 antibody. Immunocomplexes were bound to sepharose beads and incubated with recombinantly expressed Sch9-His. After extensive washing, western blot analysis of bound proteins was performed (Fig. 3 A). Beads without addition of anti-Cst6 antibody did not show a signal for either Cst6 or Sch9. Addition of Sch9-His without prior binding of Cst6 by antibodies did also not exhibit any signal, which excluded the possibility of unspecific binding. Importantly, when Cst6 was previously bound by anti-Cst6 antibody we could detect specific binding of Sch9, thus demonstrating the ability of Sch9 to bind its expected substrate ScCst6.

To provide further evidence that Sch9 is the Cst6 kinase we carried out phosphorylation experiments. We overexpressed Sch9-His in *S. cerevisiae* under control of the inducible Sc*GAL1* promoter. Sch9 expression was induced by shifting the cells from glucose to galactose containing medium. *S. cerevisiae* overexpressing cells were cultivated in 5% CO_2, assuming that the kinase should be most active

under this condition. ScSch9-His was purified from cell lysate via immunoprecipitation. Successful purification was followed by western blot analysis resulting in a strong single band at ~120 kDa in the bead-bound fraction (Fig. 3 B, left panel). Immunocomplexes with bound kinase were used for radioactive kinase assay. The substrate Cst6-His was recombinantly expressed and purified using affinity chromatography. Purity was verified with Coomassie staining, represented by a single band at ~70 kDa (Fig. 3 B, left panel). Sch9-His and Cst6-His were incubated in the presence of [γ-^{32}P] ATP before separation by 4-20% SDS-PAGE. By means of autoradiography, incorporation of γ-^{32}P was visualized. In control experiments, where the putative kinase ScSch9 was absent, no definite bands were visible, but a high background corresponding to non-incorporated radioactivity (Fig. 3 B, right panel). If Sch9 was present, two distinct bands of ~70 kDa and ~120 kDa were apparent, representing Cst6 and Sch9 respectively. These data demonstrate the phosphorylation of Cst6 by Sch9 *in vitro* and furthermore imply an extensive autophosphorylation of ScSch9, which was previously reported by Huber et al. (25).

Cst6 phosphorylation analysis demonstrates that CO_2 signals via phosphorylation of S266

CO_2 regulation of fungal CA expression is conserved and *S. cerevisiae* Cst6 is an orthologue to Rca1 in *C. albicans* and *C. glabrata*. Accordingly we hypothesized that fungal CO_2 sensing signals via phosphorylation of defined Cst6/Rca1 amino acid residues. Comparison of the Cst6/Rca1 protein sequences identified three conserved serine residues at positions S124, S126 and S222 in *C. albicans* Rca1 corresponding S266, S268 and S440 in *S. cerevisiae* Cst6. Previous work suggested that S124 but not S126 or S222 disrupts CA regulation in *C. albicans* (17). Hence, we assumed

that phosphorylation of S124 regulates fungal CO_2 sensing. In order to analyze phosphorylation probability of the three serine residues we overexpressed Cst6-His in *S. cerevisiae* WT in 5% CO_2 assuming that phosphorylation status is at maximum. Cst6-His was affinity purified via immobilized metal ion affinity chromatography (IMAC) and subjected to 4-20% SDS-PAGE. Total protein was Coomassie stained, corresponding bands were excised and Trypsin-LysC, AspN, LysargiNase or GluC digestion was performed to achieve high sequence coverage. In addition, an in-solution digestion with Trypsin-LysC and GluC was done to detect also peptides of extended length. Phosphopeptides were enriched using TiO_2 and analyzed by LC-MS/MS. Our results clearly showed that multiple sites of the Cst6 protein can be subject of phosphorylation. In WT, we detected 19 different phosphorylation sites in at least two independent experiments (Fig. 4A). Thereof, 11 residues were previously identified in high-throughput approaches (26, 27). We identified another 8 sites, which were unknown to be phosphorylated, printed in bold in Fig. 4. In *CST6*, the conserved serine residues correspond to S266, S268 and S440. Of those, only serine at position 266 was found to be phosphorylated in *S. cerevisiae* in 5% CO_2, while S268 and S440 were found to be unphosphorylated. In addition, the number of detected phosphorylations suggests the possibility of additional kinases being involved in regulation of Cst6, although we cannot draw any conclusions about biological relevance from the phosphorylation site mapping.

S266 is the only residue within Sc*CST6* matching the Sch9 consensus motif R-(R/K)-X-S (28). Hence, we mutated serine at position 266 to alanine (S266A) or aspartic acid (S266D) and cloned these sequences or WT *CST6* into *cst6*Δ to prove influence on Sc*NCE103* expression. *cst6*Δ reverted with WT *CST6* showed Sc*NCE103* expression comparable to WT (Fig. 4B). Phosphoablative mutation of S266 to A led

to a significant upregulation of Sc*NCE103* ^{CO2} (2.73 ± 0.43) while Sc*NCE103* ^{air} (6.52 ± 2.12) expression was unaltered. Interestingly, *cst6*Δ + *CST6* ^{S266A} corresponds to the expression pattern of *sch9*Δ. This confirms our hypothesis and emphasizes S266 to be phosphorylated in 5% CO_2 in order to inhibit *NCE103* expression. Phosphomimetic mutation of *CST6* (*CST6* ^{S266D}) led to slightly decreased Sc*NCE103* ^{air} expression in comparison to WT *CST6*, but differences were not statistically significant. This might point to alternative regulation mechanisms regulating *NCE103* expression, especially in air condition.

CO_2 sensing is conserved in yeast

Our findings and previous work suggest that CO_2-dependent regulation mediated via Cst6/Rca1 is conserved in some yeast species (17, 18). Due to the closer phylogenetic relationship between *S. cerevisiae* and *C. glabrata*, we first analyzed the influence of Cg*SCH9* on Cg*NCE103* expression in changing CO_2 conditions. Expression of Cg*NCE103* in 5% CO_2 and air after 60 min was quantified with qRT-PCR according to the previously described protocol for *S. cerevisiae* (Fig. 5 A). *C. glabrata* control strain, AFG1, revealed a 2-fold increase of Cg*NCE103* ^{air} compared to Cg*NCE103* ^{CO2} expression. This increase was completely absent in *rca1*Δ. In fact, Cg*NCE103* expression of *rca1*Δ was in air as low as in 5% CO_2. This is in contrast to the *S. cerevisiae cst6*Δ regulation pattern, where at least a small upregulation in air was observed. As expected, deletion of Cg*Sch9* led to significantly elevated Cg*NCE103* ^{CO2} levels (2.02 ± 0.43) compared to control. Noteworthy and in contrast to the pattern found in *S. cerevisiae,* Cg*NCE103* ^{air} expression was also increased. However, despite these differences, Sch9 clearly affects *NCE103* regulation in *C. glabrata*.

We also verified influence of *SCH9* on *C. albicans NCE103* using similar protocols (Fig. 5 B). *C. albicans* WT exhibited a 4.6-fold increase of Ca*NCE103* expression in cells transferred to air conditions. In comparison, deletion of Ca*RCA1* resulted in significant lower Ca*NCE103* ^{air} expression. A *C. albicans sch9*Δ mutant strain (24) showed significantly increased Ca*NCE103* ^{CO2} expression (2.61 ± 0.16), similar to the effects of *SCH9* deletion in *S. cerevisiae* and *C. glabrata*. Remarkably, also Ca*NCE103* ^{air} levels were elevated, which coincide to what we found for *C. glabrata*, but not for *S. cerevisiae*. Taken together these findings clearly indicate a conserved mechanism of CO_2 adaptation in pathogenic and nonpathogenic yeast species and emphasize Sch9 is key to CO_2 sensing in all three species.

Lipid signaling via Pkh1/2 but not TORC1 regulates fungal CO_2 sensing

Previous work showed that in *S. cerevisiae* Sch9 is regulated by target-of-rapamycin-complex 1 (TORC1) and homologues of the mammalian 3-phosphoinositide-dependent protein kinase (mPDK1), Pkh1/Pkh2, which phosphorylate Sch9 at specific sites (29, 30). TORC1 phosphorylates at least 6 residues of Sch9 (S711, T723, S726, T737, S758, S765) (31) while ScPkh1/2 phosphorylates Sch9 at the *PDK1* site T570 (32).

Analysis of LC-MS/MS data of overexpressed Sc*CST6*-His allowed us to detect phosphorylated peptides specific for endogenous ScSch9. This enabled analysis of Sch9 phosphorylation *in vivo* to draw conclusions about putative activators. We detected the *PDK1* site T570 and 3 of the phosphorylation sites addressed by TORC1 (S726, S758, S765) to be phosphorylated in 5% CO_2 (Fig. 6A). Therefore, we hypothesized that TOR and lipid signaling is involved in fungal CO_2 sensing and

264 that loss or inhibition of Sch9 upstream regulators mimics *sch9*Δ. Because activation
265 of Sch9 is especially important under 5% CO_2, we concentrated on changes of
266 *NCE103* ^{CO2} expression (see supplemental table S2 and S4 for *NCE103* ^{air}
267 expression). Notably, *tor1*Δ had been included in our initial qRT-PCR screening and
268 showed slightly but not significantly increased CA expression in high CO_2 (Fig. 6 B).
269 Catalytic subunits of TORC1 are either ScTor1 or ScTor2 and TORC1 is inhibited by
270 rapamycin (33). Since Tor2 is an essential gene in *S. cerevisiae* we investigated the
271 impact of TORC1 signaling on fungal CO_2 sensing via Sch9 by using rapamycin.
272 Inhibition of TORC1 by rapamycin aggravated the effect of *tor1*Δ on CA gene
273 expression and led to a significant upregulation of *NCE103* ^{CO2} (1.85 ± 0.46, Fig. 6
274 B). However, it did clearly not reach the *NCE103* ^{CO2} levels of *sch9*Δ. Single mutants
275 of Pkh1/Pkh2 did not alter *NCE103* ^{CO2} expression (Fig. 6 B), probably because of
276 Pkh1/2 redundancy in *S. cerevisiae* (34). As a conventional double Pkh1/2 deletion
277 mutant is known to be lethal in *S. cerevisiae* (35), we used a temperature-sensitive
278 double mutant (35) to investigate the influence of Pkh1/2 mediated activation of Sch9
279 on *NCE103* ^{CO2} expression. Indeed, expression levels of *NCE103* ^{CO2} increased
280 significantly to 2-fold in *pkh1*^{ts} *pkh2*Δ compared to its control strain 15 Dau. This
281 implies, that Sch9 mediated effects on CA expression could be dependent on both
282 Sch9 regulators, TORC1 and Pkh1/2.

283 To analyze influence of Sch9 activation by TORC1 and Pkh1/2 more precisely, we
284 investigated *NCE103* expression of strains with site-specific mutations of known
285 Sch9 phosphorylation sites addressed by TORC1 and Pkh1/2. As control, *sch9*Δ
286 reverted with WT *SCH9* was used, which showed comparable *NCE103* expression
287 levels in 5% CO_2 and air as WT strain. Surprisingly, also phosphoablative mutation of
288 all 6 TORC1 sites (S711A, T723A, S726A, T737A, S758A, S765A), referred to as

289 *SCH9* ^{6A}, resulted in WT-like *NCE103* expression levels (Fig. 6C). In contrast, T570A
290 mutation of the *PDK1* site resulted in significantly elevated Sc*NCE103* ^{CO2} expression
291 (2.7 ± 0.59), while Sc*NCE103* ^{air} expression was not changed.This is comparable
292 with the deregulation pattern of *sch9*Δ. Additional S/T to A mutation of the 6 TORC1
293 sites within *SCH9* (*SCH9* $^{T570A,\ 6A}$), showed no additive effect on Sc*NCE103*
294 expression (Fig. 6C).

295 Taking all together, we concluded that phosphorylation of Sch9 by Pkh1/2 at T570 is
296 crucial for Sch9 activation in 5% CO_2 environment in order to decrease Sc*NCE103*
297 expression. Although phosphorylation sites addressed by TORC1 were detected in
298 Sch9, CO_2-dependent activation of Sch9 and, thus, CO_2 adaptation seems to be
299 independent of TORC1.

300

301 **Discussion**

302 Sensing and adapting to alterations in ambient CO_2 is of paramount importance for
303 all living organisms. Fungi adjust their metabolism to CO_2 availability and CA are
304 essential in this process. CA catalyze the reversible conversion of mobile CO_2 to
305 HCO_3^- and disruption of their function using CA inhibitors or deletion distorts fungal
306 metabolism or abolishes growth altogether.

307 Expression of the fungal CA *NCE103* is regulated by the transcription factor
308 Cst6/Rca1, which belong to the ATF/CREB family (17). To identify enzymes
309 responsible for Cst6/Rca1 phosphorylation, and unravel fungal CO_2 sensing, we
310 screened a kinase/phosphatase mutant library in the model organism *S. cerevisiae*.
311 The library consisted of 111 kinase and 44 phosphatase mutants and Sch9 was the
312 most promising identified kinase candidate.

313 Sch9 regulates ribosome biogenesis, cell cycle progression and lifespan and is
314 involved in heat shock, osmotic and oxidative stress response by integrating nutrient
315 signals (20-23, 36-38). Several lines of evidence support our hypothesis that Sch9 is
316 indeed the Cst6 kinase and relays fungal CO_2 sensing: Immunoprecipitation using
317 endogenous Cst6 showed physical interaction between Cst6 and Sch9. Furthermore,
318 *in vitro* phosphorylation showed that Sch9 mediates the incorporation of radioactively
319 labeled phosphate groups into Cst6, clearly demonstrating the kinase activity. Finally,
320 the preferred consensus motif for Sch9 phosphorylation events is R-(R/K)-X-S (28).

321 Our work provides evidence that regulation of *NCE103* in *S. cerevisiae, C. glabrata*
322 and *C. albicans* is conserved. Deletion of Sc*SCH9,* Cg*SCH9* and Ca*SCH9* affected
323 *NCE103* expression in a comparable way as they lead to a significant upregulation of
324 *NCE103* ^{CO2} (Fig. 1 and Fig. 5). Previous work provided some indirect evidence
325 suggesting that S124 in *C. albicans* may be subject to phosphorylation impacting on
326 Rca1/Cst6 function (17). S124 is conserved in *S. cerevisiae* (corresponding position
327 S266) and *C. glabrata* Rca1 (S387). We now show proof that S266, but not other
328 candidate residues, are phosphorylated in *CST6* in elevated CO_2 and thus provide a
329 molecular explanation for the conservation of CO_2 signaling in yeast (Fig. 4).
330 Furthermore, we showed that phosphorylation of Sc*CST6* at S266 is crucial for
331 repression of *NCE103* ^{CO2}, because the phosphoablative mutation S266A resulted in
332 increased *NCE103* ^{CO2} expression. This is in accordance with the results Cottier et
333 al. found for S124 in *C. albicans* Rca1 (17).

334 Sch9 is a member of the AGC family (homologous to protein kinases A, G and C) of
335 proteins. It is conserved in *S. cerevisiae*, *C. glabrata* and *C. albicans* but is also
336 found in less related fungal species like *Fusarium graminearum* (39). In mammalian
337 cells it has been hypothesized that PKB/Akt is the Sch9 homologue (40) although

later studies suggest that Sch9 is more closely related to S6K1 (31) which acts downstream of TORC1. The best characterized regulator of CA in human cells is HIF-1α, which induces human CA IX expression in response to hypoxia (41, 42). HIF-1α has been found to be regulated by mTOR, which suggested the assumption that Cst6/Rca1 regulation in yeast is also TOR-dependent. Surprisingly, our experiments demonstrated that Sch9 phosphorylation by TORC1 does not contribute to CO_2 dependent *NCE103* regulation (Fig. 6C). Indeed, inhibition of TORC1 by rapamycin showed effects on *NCE103* ^{CO2} (Fig. 6B), but these effects seem not to be dependent on Sch9 signaling. Furthermore, it was shown that addition of rapamycin is not always similar to inhibition of TORC1 (43). Instead of TORC1, phosphorylation by Pkh1/2 at T570 seems to be the driving force for Sch9 activation in order to repress *NCE103* expression in 5% CO_2 (Fig. 7). It should be considered that Pkh1/2 might not be the sole activator of Sch9. Deletion of *SCH9* results in a 3.55-fold upregulation of Sc*NCE103* ^{CO2}, whereas increase following deletion of *PKH1/2* was only 1.93. Also T570A mutation of Sch9 leading to unresponsiveness to Pkh1/2 activation did not reach that high *NCE103* ^{CO2} levels. Thus, there is the possibility that Sch9 is directly influenced by CO_2 levels and not only via Pkh1/2 (Fig. 7). An influence of oxygen levels on Sch9 activity should also be considered as it has been previously reported that Sch9 inhibits hyphae formation in the fungal pathogen *C. albicans* at high CO_2 conditions (>1%) and hypoxia (<10%), but neither condition alone (24).

It is noteworthy that another candidate identified in our screen was ScTpd3, which is a part of the protein phosphatase 2A complex. Although no kinase function has been reported, the protein phosphatase 2A complex is linked to nutrient signaling via Tor (44) and is suspected to dephosphorylate Sch9. Overexpression of Sc*TPD3* and

362 deletion of *SCH9* result in comparable phenotypes (45). Thus, ScTpd3 might indeed
363 play a role in *NCE103* regulation, maybe as regulator of ScSch9.

364 The complexity of *NCE103* regulation is further confirmed by our finding that despite
365 the absence of ScCst6 as transcriptional activator, we could observe upregulation of
366 Sc*NCE103* ^{air} resulting in elevated ScNce103p, although this was clearly less
367 pronounced than in WT (Fig. 2 A). Therefore, besides the ScSch9-ScCst6 pathway,
368 there seems to be other mechanisms regulating Sc*NCE103*, maybe another – so far
369 unknown - transcription factor (Fig. 7 B). This could be an explanation for the viability
370 of *cst6*Δ mutants even under air conditions whereas *nce103*Δ mutants are only able
371 to grow in elevated CO_2 environment (16). Only a moderate induction of *NCE103*
372 expression seems to be sufficient for fungal survival, but it will result in growth delay
373 and, probably, affect other cell properties.

374 We provide insight into fungal CO_2 sensing and show that lipid signaling activating
375 Pkh1/2 regulate metabolic adaptation via Sch9. More work is needed to identify the
376 precise molecular events and complex feedback mechanisms involved in CO_2 signal
377 reception and transduction to Sch9. However, the Sch9-Cst6/Rca1 cascade is
378 conserved in yeast and central to fungal metabolism and Rca1 has previously been
379 reported to play a role in biofilm formation, which is instrumental in fungal
380 pathogenesis (46). Thus, targeting fungal specific components in organisms CO_2
381 sensing, such as CA or Rca1/Cst6, constitutes a valid approach to new treatment
382 option.

383

Materials and Methods

Strains, plasmids, primer

See supplemental table S1

Sc*NCE103* expression analysis

Exponential cultures of *S. cerevisiae* WT (BY4741) were cultivated at 37°C as duplicates in 5% CO_2 and transferred to air for 10, 30, 60, 90, 120 or 180 min to induce Sc*NCE103* expression. Pellets were harvested and RNA was extracted using a hot phenol chloroform method (47). Quantity of RNA was measured with NanoDrop 2000 (Thermo Fisher Scientific, Waltham, Massachusetts) and 100 ng/µl RNA were utilized as template for qRT-PCR using the Brilliant III Ultra Fast SYBR Green qRT PCR Kit on a Stratagene Mx3005P (both Agilent Technologies, Santa Clara, California). Gene expression was calculated with the ΔΔCt method (48) using Sc*ACT1* as housekeeping gene. The same procedure was done for the screening of *S. cerevisiae* kinase/phosphatase mutant library (Euroscarf, Frankfurt, Germany). Exponential cultures were transferred to air for 60 min to induce highest Sc*NCE103* expression. Sc*NCE103* expression of mutants was normalized to WT expression in 5% CO_2 (supplemental Fig. S2). Mutants were tested at least twice, those, which showed dysregulation were run 3 to 6 times. Expression of WT strain was measured in every qRT-PCR as internal control. For rapamycin experiments, 200 nM rapamycin of a 1 mM stock solution in DMSO was added. DMSO served as solvent control. Sc*NCE103* expression of strains 15 Dau and *pkh1* ^{ts} *pkh2*Δ was measured with slight differences in the protocol due to temperature sensitivity of *pkh1* ^{ts} *pkh2*Δ. Strains were preincubated overnight in 30°C and 5% CO_2 and transferred to 37°C for 3h to

409 inhibit Pkh1 synthesis. Then samples were transferred to air for another hour to
410 induce Sc*NCE103*.

411

412 **Expression and purification of His-tagged proteins from *E. coli***

413 *S. cerevisiae CST6*, *NCE103* and *SCH9* were synthesized with a C-terminal 6xHis
414 tag (GeneArt Gene Synthesis, Thermo Fisher Scientific) and cloned into *E. coli*
415 expression vector p41. *NCE103* and *SCH9* were expressed in *E.coli* strain BL21DE3
416 (New England Biolabs, Ipswich, Massachusetts). Bacteria were grown in LB medium
417 (10 g/l NaCl, 5 g/l yeast extract, 10 g/l tryptone, pH 7) with 50 µg/ml ampicillin at
418 37°C. Sc*NCE103* expression was induced with 1 mM IPTG at OD_{600} 0.2 and
419 cultivated overnight until harvesting. Expression of Sc*SCH9* was induced at OD_{600}
420 0.8 for 4 h at RT. Sc*CST6* expression was performed using *E.coli* Rosetta. Cells
421 were cultivated in LB medium with 50 µg/ml ampicillin and 34 µg/ml chloramphenicol
422 at 37°C until OD_{600} 0.4. Expression was induced with 1 mM IPTG for 4 h at 37°C.
423 Bacteria were harvested, resuspended in purification buffer (25 mM sodium
424 phosphate pH 7.4, 250 mM NaCl, 10 mM imidazole, 1 mM PMSF) and disrupted by
425 freeze and thaw for a total of 3 rounds. Recombinant proteins were purified by IMAC
426 using Ni-NTA sepharose (Biozol, Eching, Germany). His-tagged proteins were eluted
427 with purification buffer, containing 250 mM imidazole. For further purification of
428 ScCst6-His, size exclusion chromatography using an ÄKTA with a Sephadex 200 GL
429 column (both GE Healthcare, Little Chalfont, United Kingdom) was performed.
430 Protein purity was determined by silver staining and quantity was measured with
431 BCA assay. At least 1 mg purified protein was used to produce specific rabbit
432 antibodies against ScCst6-His and ScNce103-His (Thermo Fisher Scientific).

433

Western blot analysis

For detection of ScNce103 levels, 10 ml of *S. cerevisiae* exponential cultures were cultivated in 5% CO_2 or transferred to air for 90 min. Cells were harvested, resuspended in 500 µl yeast lysis buffer (50 mM Tris/HCl, 150 mM NaCl, 0.1% Triton X-100, 1 mM DTT, 10% glycerol, PhosStop, Complete protease inhibitor EDTA-free, PMSF) and lysed with glass beads (diameter: 425-600 µm) for 5× 1 min with incubation on ice in between. Lysates were centrifuged (16000 g, 10 min, 4°C) and total protein was measured using BCA protein assay kit (Thermo Fisher Scientific). After addition of 5x SDS loading dye and heating at 95°C for 5 min, samples (1 mg total protein) were subjected to 4-20% SDS-PAGE. Transfer to PVDF membrane was performed using Bio-Rad Wet/Tank blotting system for 1 h. 3% nonfat dry milk in TBS was used for membrane blocking and antibody binding. Membranes were incubated with custom made rabbit anti-ScNce103 (1:1000, Thermo Fisher Scientific) and mouse anti-beta Actin (ab8224, 1:1000, abcam, Cambridge, UK) overnight at 4°C with gentle rotation. After incubation with fluorophore-labeled secondary antibodies (Jackson ImmunoResearch, West Grove, Pennsylvania) for 2 h at 4°C, signals were detected with FluorChem Q Imager (Alpha innotec, Kasendorf, Germany). Quantitative analysis was done using the AlphaView Software (ProteinSimple).

NCE103 promoter driven GFP expression

S. cerevisiae WT, *cst6Δ* and *sch9Δ* were transformed with pRS316 plasmid, containing GFP under control of Sc*NCE103* promoter using the lithium-acetate-method according to Gietz et al. (49). In brief, yeast cells of early lag phase were harvested, washed and resuspended in TE buffer with 100 mM LiAc. 50 µl cell

aliquots were incubated with heat-denatured salmon-sperm DNA and 240 µl 50% PEG 3640, then DNA was added. Samples were incubated at 30°C for 30 min. After addition of 45 µl DMSO, heat shock at 42°C for 15 min was performed. Centrifuged and resuspended cells were incubated for 2 h at 30°C and washed again before plating. Picked colonies were cultivated at 30°C overnight in 5% CO_2 in minimal medium supplemented with histidine, methionine and leucine. After inoculation of duplicates, one culture was transferred to air, while the second one was further incubated under 5% CO_2. Fluorescence was detected with LSM 780 (Zeiss, Jena, Germany) at time point of the CO_2 to air switch and after 60 and 120 min of incubation. GFP fluorescence of 50 cells per time point were measured using ZEN software (Zeiss) and mean fluorescence was calculated.

Protein expression in *S. cerevisiae*

Overexpression of Sc*CST6*-His and Sc*SCH9*-His in *S. cerevisiae* was achieved using Sc*GAL1* promoter. Yeast cells were cultivated in minimal medium, supplemented with histidine, methionine and leucine at 30°C overnight. Sc*CST6* and Sc*SCH9* overexpression was induced by a shift from minimal medium to YEP medium (1% yeast extract, 2% peptone) containing 2% raffinose and after overnight culture to YEP with 2% galactose for additional 6 h. Cells were harvested, resuspended in yeast lysis buffer and lysed with glass beads as described. Cell extracts were tested in western blot for overexpression.

Immunoprecipitation

Exponential *S. cerevisiae* WT or Sc*SCH9*-His overexpressing cultures (50 ml) were harvested, resuspended in 500 µl IP buffer (20 mM sodium phosphate pH 7, PhosStop, Complete protease inhibitor EDTA-free, PMSF) and lysed with glass beads as described. Extracts were incubated with either custom made rabbit anti-Cst6, saturated with 5 µg 6xHis tag peptide (GENTAUR, Aachen, Germany), or anti-6xHis antibody (GTX115045, GeneTex, Hsinchu City, Taiwan) overnight at 4°C. 50 µl protein-G sepharose beads (GE Healthcare) were washed with IP wash buffer (IP buffer + 500 mM NaCl) and incubated with immunocomplexes for 1 h at 4°C. Beads were centrifuged at 2500 rpm for 2 min, supernatant was taken off with a syringe and a 25G needle, and beads were resuspended in wash buffer and incubated 1 min with shaking. This washing procedure was repeated four times. For co-IP, beads were furthermore incubated with 20 µg recombinant ScSch9-His lysate for 3 h at 4°C. After extensive washing, beads were boiled in SDS sample buffer, subjected to 4-20% SDS-PAGE and analyzed using western blot. Rabbit anti-ScCst6 (1:1000) was used for detection of endogenous ScCst6 and FITC-labeled mouse anti-6xHis (MA1-81891, 1:250, Thermo Fisher Scientific) for detection of 6x His-tagged ScSch9.

Radioactive kinase assay

ScSch9-His was immunoprecipitated from *S. cerevisiae* Sc*SCH9*-His overexpressing culture. After washing of bead-bound immunocomplexes with IP wash buffer, an additional washing step with 1x kinase buffer (PBS pH 7.4, 4 mM MgCl, 10 mM DTT, 20% glycerol, 1 mM PMSF) was performed. 1 µg bacterially expressed and purified ScCst6-His was added to immunocomplexes in 50 µl kinase buffer. After addition of 100 µM ATP and 25 µCi [γ-^{32}P] Adenosine 5'-triphosphate (PerkinElmer, Waltham, Massachusetts, BLU002250UC, specific activity: 10 Ci/mmol), reactions were

incubated at 30°C for 30 min. Kinase reaction was stopped by heating at 95°C for 5 min in 4x SDS loading dye and samples were subjected to 4-20% SDS-PAGE. Gels were dried and radioactive incorporation was detected by autoradiography.

Liquid chromatography coupled to tandem mass spectrometry (LC-MS/MS) analysis and protein database search

To detect CO_2-dependent phosphorylation in ScCst6, Sc*CST6* overexpressing *S. cerevisiae* cultures were were harvested and ScCst6-His was purified using IMAC. For mass spectrometry analysis, in-gel digest with Trypsin-LysC, AspN, GluC (all Promega, Madison, Wisconsin) or LysargiNase (50) and in-solution digest with Trypsin-LysC and GluC was performed. Peptides were extracted with trifluoroacetic acid and increasing concentrations of acetonitrile (50-90%) after in-gel digestion. Phosphopeptide enrichment was carried out using the TiO_2 method (TiO_2 Spin Tip Sample Prep Kit, protea Biosciences, Morgantown, West Virginia) and remaining peptides were purified with C18 mini columns (C18 Spin Tip Sample Prep Kit, protea Biosciences, Morgantown, West Virginia). Dried peptides were solubilized in MS buffer (0.05% trifluoroacetic acid in 2% acetonitril/98% H_2O) and applied to LC-MS/MS analysis, carried out on an Ultimate 3000 nano RSLC system coupled to a QExactive Plus mass spectrometer (both Thermo Fisher Scientific). Thermo raw files were processed via the Proteome Discoverer (PD) v1.4.0.288. Tandem mass spectra were searched against the NCBI protein database of *S. cerevisiae* using the algorithms of Mascot v2.4.1 (Matrix Science, London, UK), Sequest HT and MS Amanda. For further information see supplemental experimental procedures.

Site-specific mutagenesis of Sc*CST6* and Sc*SCH9*

Phosphoablative (S266A) and phosphomimetic (S266D) sequences of Sc*CST6* (GeneArt Gene Synthesis) were inserted in pRS316 plasmid using PacI/AscI restriction sites. The Sc*CST6* promoter was cloned in pRS316 using SacI/PacI. After transformation of *S. cerevisiae cst6*Δ, Sc*NCE103* expression in 5% and 0.04% CO_2 was measured as described and normalized to WT expression in 5% CO_2. For construction of Sc*SCH9* with S/T to A mutation of all 6 TORC1 sites (*SCH9* ^{6A}), the sequence of *SCH9* $^{T570A,\ 6A}$ was used as template. A570 was remutated to T570 using QuikChange II Site-Directed Mutagenesis Kit (Agilent Technologies) with mutation-specific primers. The plasmid with the corrected sequence was checked via sequencing and used for transformation of *sch9*Δ.

Construction of *C. glabrata sch9*Δ mutant

Deletion of Cg*SCH9* was achieved by replacement of Cg*SCH9* ORF by *NAT1* cassette, which mediates resistance against nourseothricin. *NAT1* was amplified by PCR with EcoRI/SacI restriction sites and cloned into pBluescript. A homologous region upstream of Cg*SCH9* ORF with a length of 1000 bp was amplified by colony-PCR and cloned into pBluescript using KpnI/XhoI. The same was done for a 1000 bp fragment located downstream of Cg*SCH9* ORF using restriction sites SacII/SacI. The whole construct, the *NAT1* cassette flanked by homologous regions, was restricted with KpnI/SacI and purified in order to transform *C. glabrata.* AFG1, a strain lacking *LIG4*, was used for transformation because of its increased efficiency of homologous recombination (51). Transformation was performed using the lithium-acetate-method, plated on YPD with 100 µg/ml ClonNAT and positive clones were selected. Integration of *NAT1* cassette and deletion of Cg*SCH9* was checked by colony-PCR

with specific internal primers. Furthermore, deletion mutants were verified using external primers (supplemental Fig. S3).

NCE103 expression measurement of *C. glabrata* and *C. albicans*

Measurement of Cg*NCE103* and Ca*NCE103* expression was performed according to the protocol for Sc*NCE103* expression, described in the first section. As housekeeping genes, Cg*ACT1* for Cg*NCE103* and Ca*ACT1* for Ca*NCE103* measurement were used.

Statistical analysis

Data are presented as arithmetic means ± standard deviation and statistical significance ($p<0.05$) was calculated using a two-sided t-test for unpaired samples.

Funding information

This work was funded by the Deutsche Forschungsgemeinschaft DFG (KU1540/3-1 to OK). Work in the lab of AB, OKn and TK was funded by the Deutsche Forschungsgemeinschaft within the Collaborative Research Center TR124 (project A1 and Z2).

Acknowledgements

We thank Dr. Robbie Loewith (University of Geneva, Switzerland) for providing Sc*SCH9* plasmids pRS416-promScSCH9-ScSCH9-3HA, pRS416-promScSCH9-ScSCH9-3HA (T570A), pGEX-6P-1 ScSCH9-3HA (S711A, T723A, S726A, T737A, S758A, S765A) and pRS416-promScSCH9-ScSCH9-3HA (T570A, S711A, T723A, S726A, T737A, S758A, S765A). Furthermore, we are grateful to Cindy Reichmann for expert technical assistance and Ilaria Granata for help with the library screening.

Author contributions

SP, RM, DH, TK, FH performed experiments and analyzed data; OKn, HPS, AB, PVD, JFE, FM, OK contributed strains and reagents and interpreted data; FM, OK designed experiments; SP, FM, OK wrote the manuscript.

Conflict of interest

The authors declare that they have no conflict of interest.

Supplemental information

Table S1

Strains, plasmids and primers used in the study

Table S2

Mean Sc*NCE103* expression and standard deviation (SD) of *S. cerevisiae* kinase/phosphatase mutants in changing CO_2 environment

Table S3

Kinase candidate genes identified in mutant library screening

Table S4

Mean Sc*NCE103* expression and standard deviation (SD) of *S. cerevisiae SCH9* regulator mutants and *S. cerevisiae* under rapamycin treatment

Fig. S1 CO_2-dependent time-course expression of Sc*NCE103* and Sc*CST6*

S. cerevisiae wild type was grown in 5% CO_2 to exponential phase and either stayed at 5% CO_2 or transferred to air. Sc*NCE103* (A) and Sc*CST6* (B) time-course expression was measured with qRT-PCR and normalized to expression at time point 0 in 5% CO_2. Sc*NCE103* mRNA levels increase significantly in air, the highest expression was measured after 60 min. In contrast, Sc*CST6* expression is independent of CO_2 levels. The graphs show means ± standard deviation. Significance against expression in 5% CO_2 was defined as * $p \leq 0.05$ and ** $p \leq 0.01$. n=3

Fig. S2 Workflow of mutant library screening for Cst6 kinase identification

S. cerevisiae wild type and deletion mutants were grown in 5% CO_2 to exponential phase and either stayed at 5% CO_2 or transferred to air for 60 min. RNA was extracted and Sc*NCE103* expression was analyzed with qRT-PCR. Data were normalized to WT expression in 5% CO_2. Putative Cst6 kinase deletion mutants were identified according to elevated Sc*NCE103* expression in 5% CO_2 compared to WT.

Fig. S3 Verification of *C. glabrata sch9* deletion

(A) Insertion of *NAT1* and deletion of Cg*SCH9* were analyzed with colony-PCR of untransformed parental strain (AFG1) and *sch9* mutant. For amplification of *NAT1*, internal primers G1-CgSCH9 and X2-NAT1 were used, for amplification of Cg*SCH9* G1-CgSCH9 and I2-CgSCH9. The strain AFG1 showed no signal for *NAT1*, but for *SCH9*. In contrast, *sch9* deletion mutant exhibited a PCR product for *NAT1*, but not for *SCH9*. As marker, GeneRuler 1 kb DNA Ladder (Thermo Fisher Scientific) was used in lane 1.

(B) For verification of correct position of *NAT1* cassette insertion, PCR with external primers G1-CgSCH9 and G4-CgSCH9 were used, which bind outside of the inserted cassette. If *SCH9* ORF is present, a PCR product of 4385 bp occurs. If *SCH9* ORF is replaced by *NAT1*, a shift to 3463 bp is visible. As marker, GeneRuler 1 kb DNA Ladder (Thermo Fisher Scientific) was used in lane 1.

Supplemental methods

Supplemental references

References

1. **Hetherington AM, Raven JA.** 2005. The biology of carbon dioxide. Curr Biol **15:**R406-410.
2. **Cummins EP, Selfridge AC, Sporn PH, Sznajder JI, Taylor CT.** 2014. Carbon dioxide-sensing in organisms and its implications for human disease. Cell Mol Life Sci **71:**831-845.
3. **Sharabi K, Lecuona E, Helenius IT, Beitel GJ, Sznajder JI, Gruenbaum Y.** 2009. Sensing, physiological effects and molecular response to elevated CO2 levels in eukaryotes. J Cell Mol Med **13:**4304-4318.
4. **Bahn YS, Muhlschlegel FA.** 2006. CO2 sensing in fungi and beyond. Curr Opin Microbiol **9:**572-578.
5. **Frame GW, Strauss WG, Maibach HI.** 1972. Carbon dioxide emission of the human arm and hand. J Invest Dermatol **59:**155-159.
6. **Polke M, Hube B, Jacobsen ID.** 2015. Candida survival strategies. Adv Appl Microbiol **91:**139-235.
7. **Brunke S, Hube B.** 2013. Two unlike cousins: Candida albicans and C. glabrata infection strategies. Cell Microbiol **15:**701-708.
8. **Klengel T, Liang WJ, Chaloupka J, Ruoff C, Schroppel K, Naglik JR, Eckert SE, Mogensen EG, Haynes K, Tuite MF, Levin LR, Buck J, Muhlschlegel FA.** 2005. Fungal adenylyl cyclase integrates CO2 sensing with cAMP signaling and virulence. Curr Biol **15:**2021-2026.
9. **Rocha CR, Schroppel K, Harcus D, Marcil A, Dignard D, Taylor BN, Thomas DY, Whiteway M, Leberer E.** 2001. Signaling through adenylyl cyclase is essential for hyphal growth and virulence in the pathogenic fungus Candida albicans. Mol Biol Cell **12:**3631-3643.
10. **Alspaugh JA, Pukkila-Worley R, Harashima T, Cavallo LM, Funnell D, Cox GM, Perfect JR, Kronstad JW, Heitman J.** 2002. Adenylyl cyclase functions downstream of the Galpha protein Gpa1 and controls mating and pathogenicity of Cryptococcus neoformans. Eukaryot Cell **1:**75-84.
11. **Amoroso G, Morell-Avrahov L, Muller D, Klug K, Sultemeyer D.** 2005. The gene NCE103 (YNL036w) from Saccharomyces cerevisiae encodes a functional carbonic anhydrase and its transcription is regulated by the concentration of inorganic carbon in the medium. Mol Microbiol **56:**549-558.
12. **Aguilera J, Petit T, de Winde JH, Pronk JT.** 2005. Physiological and genome-wide transcriptional responses of Saccharomyces cerevisiae to high carbon dioxide concentrations. FEMS Yeast Res **5:**579-593.
13. **Supuran CT.** 2008. Carbonic anhydrases--an overview. Curr Pharm Des **14:**603-614.
14. **Aguilera J, Van Dijken JP, De Winde JH, Pronk JT.** 2005. Carbonic anhydrase (Nce103p): an essential biosynthetic enzyme for growth of Saccharomyces cerevisiae at atmospheric carbon dioxide pressure. Biochem J **391:**311-316.
15. **Elleuche S, Poggeler S.** 2010. Carbonic anhydrases in fungi. Microbiology **156:**23-29.
16. **Gotz R, Gnann A, Zimmermann FK.** 1999. Deletion of the carbonic anhydrase-like gene NCE103 of the yeast Saccharomyces cerevisiae causes an oxygen-sensitive growth defect. Yeast **15:**855-864.
17. **Cottier F, Raymond M, Kurzai O, Bolstad M, Leewattanapasuk W, Jimenez-Lopez C, Lorenz MC, Sanglard D, Vachova L, Pavelka N, Palkova Z, Muhlschlegel FA.** 2012. The bZIP transcription factor Rca1p is a central regulator of a novel CO(2) sensing pathway in yeast. PLoS Pathog **8:**e1002485.
18. **Cottier F, Leewattanapasuk W, Kemp LR, Murphy M, Supuran CT, Kurzai O, Muhlschlegel FA.** 2013. Carbonic anhydrase regulation and CO(2) sensing in the fungal pathogen Candida glabrata involves a novel Rca1p ortholog. Bioorganic & medicinal chemistry **21:**1549-1554.
19. **Garcia-Gimeno MA, Struhl K.** 2000. Aca1 and Aca2, ATF/CREB activators in Saccharomyces cerevisiae, are important for carbon source utilization but not the response to stress. Mol Cell Biol **20:**4340-4349.

20. **Morano KA, Thiele DJ.** 1999. The Sch9 protein kinase regulates Hsp90 chaperone complex signal transduction activity in vivo. EMBO J **18:**5953-5962.
21. **Pascual-Ahuir A, Proft M.** 2007. The Sch9 kinase is a chromatin-associated transcriptional activator of osmostress-responsive genes. EMBO J **26:**3098-3108.
22. **Weinberger M, Mesquita A, Caroll T, Marks L, Yang H, Zhang Z, Ludovico P, Burhans WC.** 2010. Growth signaling promotes chronological aging in budding yeast by inducing superoxide anions that inhibit quiescence. Aging (Albany NY) **2:**709-726.
23. **Qie B, Lyu Z, Lyu L, Liu J, Gao X, Liu Y, Duan W, Zhang N, Du L, Liu K.** 2015. Sch9 regulates intracellular protein ubiquitination by controlling stress responses. Redox Biol **5:**290-300.
24. **Stichternoth C, Fraund A, Setiadi E, Giasson L, Vecchiarelli A, Ernst JF.** 2011. Sch9 kinase integrates hypoxia and CO2 sensing to suppress hyphal morphogenesis in Candida albicans. Eukaryot Cell **10:**502-511.
25. **Huber A, Bodenmiller B, Uotila A, Stahl M, Wanka S, Gerrits B, Aebersold R, Loewith R.** 2009. Characterization of the rapamycin-sensitive phosphoproteome reveals that Sch9 is a central coordinator of protein synthesis. Genes Dev **23:**1929-1943.
26. **Swaney DL, Beltrao P, Starita L, Guo A, Rush J, Fields S, Krogan NJ, Villen J.** 2013. Global analysis of phosphorylation and ubiquitylation cross-talk in protein degradation. Nat Methods **10:**676-682.
27. **Albuquerque CP, Smolka MB, Payne SH, Bafna V, Eng J, Zhou H.** 2008. A multidimensional chromatography technology for in-depth phosphoproteome analysis. Mol Cell Proteomics **7:**1389-1396.
28. **Kennelly PJ, Krebs EG.** 1991. Consensus sequences as substrate specificity determinants for protein kinases and protein phosphatases. J Biol Chem **266:**15555-15558.
29. **Jacinto E, Lorberg A.** 2008. TOR regulation of AGC kinases in yeast and mammals. Biochem J **410:**19-37.
30. **Liu K, Zhang X, Lester RL, Dickson RC.** 2005. The sphingoid long chain base phytosphingosine activates AGC-type protein kinases in Saccharomyces cerevisiae including Ypk1, Ypk2, and Sch9. J Biol Chem **280:**22679-22687.
31. **Urban J, Soulard A, Huber A, Lippman S, Mukhopadhyay D, Deloche O, Wanke V, Anrather D, Ammerer G, Riezman H, Broach JR, De Virgilio C, Hall MN, Loewith R.** 2007. Sch9 is a major target of TORC1 in Saccharomyces cerevisiae. Mol Cell **26:**663-674.
32. **Voordeckers K, Kimpe M, Haesendonckx S, Louwet W, Versele M, Thevelein JM.** 2011. Yeast 3-phosphoinositide-dependent protein kinase-1 (PDK1) orthologs Pkh1-3 differentially regulate phosphorylation of protein kinase A (PKA) and the protein kinase B (PKB)/S6K ortholog Sch9. J Biol Chem **286:**22017-22027.
33. **Loewith R, Jacinto E, Wullschleger S, Lorberg A, Crespo JL, Bonenfant D, Oppliger W, Jenoe P, Hall MN.** 2002. Two TOR complexes, only one of which is rapamycin sensitive, have distinct roles in cell growth control. Mol Cell **10:**457-468.
34. **Casamayor A, Torrance PD, Kobayashi T, Thorner J, Alessi DR.** 1999. Functional counterparts of mammalian protein kinases PDK1 and SGK in budding yeast. Curr Biol **9:**186-197.
35. **Inagaki M, Schmelzle T, Yamaguchi K, Irie K, Hall MN, Matsumoto K.** 1999. PDK1 homologs activate the Pkc1-mitogen-activated protein kinase pathway in yeast. Mol Cell Biol **19:**8344-8352.
36. **Huber A, French SL, Tekotte H, Yerlikaya S, Stahl M, Perepelkina MP, Tyers M, Rougemont J, Beyer AL, Loewith R.** 2011. Sch9 regulates ribosome biogenesis via Stb3, Dot6 and Tod6 and the histone deacetylase complex RPD3L. EMBO J **30:**3052-3064.
37. **Huang X, Liu J, Dickson RC.** 2012. Down-regulating sphingolipid synthesis increases yeast lifespan. PLoS Genet **8:**e1002493.
38. **Jorgensen P, Rupes I, Sharom JR, Schneper L, Broach JR, Tyers M.** 2004. A dynamic transcriptional network communicates growth potential to ribosome synthesis and critical cell size. Genes Dev **18:**2491-2505.

693 39. **Chen D, Wang Y, Zhou X, Wang Y, Xu JR.** 2014. The Sch9 kinase regulates conidium size,
694 stress responses, and pathogenesis in Fusarium graminearum. PLoS One **9:**e105811.
695 40. **Sobko A.** 2006. Systems biology of AGC kinases in fungi. Sci STKE **2006:**re9.
696 41. **Wykoff CC, Beasley NJ, Watson PH, Turner KJ, Pastorek J, Sibtain A, Wilson GD, Turley H,**
697 **Talks KL, Maxwell PH, Pugh CW, Ratcliffe PJ, Harris AL.** 2000. Hypoxia-inducible expression
698 of tumor-associated carbonic anhydrases. Cancer Res **60:**7075-7083.
699 42. **Schofield CJ, Ratcliffe PJ.** 2005. Signalling hypoxia by HIF hydroxylases. Biochem Biophys Res
700 Commun **338:**617-626.
701 43. **Thoreen CC, Sabatini DM.** 2009. Rapamycin inhibits mTORC1, but not completely. Autophagy
702 **5:**725-726.
703 44. **Zabrocki P, Van Hoof C, Goris J, Thevelein JM, Winderickx J, Wera S.** 2002. Protein
704 phosphatase 2A on track for nutrient-induced signalling in yeast. Mol Microbiol **43:**835-842.
705 45. **Sugajska E, Swiatek W, Zabrocki P, Geyskens I, Thevelein JM, Zolnierowicz S, Wera S.** 2001.
706 Multiple effects of protein phosphatase 2A on nutrient-induced signalling in the yeast
707 Saccharomyces cerevisiae. Mol Microbiol **40:**1020-1026.
708 46. **Riera M, Mogensen E, d'Enfert C, Janbon G.** 2012. New regulators of biofilm development in
709 Candida glabrata. Res Microbiol **163:**297-307.
710 47. **Martin R, Moran GP, Jacobsen ID, Heyken A, Domey J, Sullivan DJ, Kurzai O, Hube B.** 2011.
711 The Candida albicans-specific gene EED1 encodes a key regulator of hyphal extension. PLoS
712 One **6:**e18394.
713 48. **Pfaffl MW.** 2001. A new mathematical model for relative quantification in real-time RT-PCR.
714 Nucleic Acids Res **29:**e45.
715 49. **Gietz D, St Jean A, Woods RA, Schiestl RH.** 1992. Improved method for high efficiency
716 transformation of intact yeast cells. Nucleic Acids Res **20:**1425.
717 50. **Huesgen PF, Lange PF, Rogers LD, Solis N, Eckhard U, Kleifeld O, Goulas T, Gomis-Ruth FX,**
718 **Overall CM.** 2015. LysargiNase mirrors trypsin for protein C-terminal and methylation-site
719 identification. Nat Methods **12:**55-58.
720 51. **Cen Y, Fiori A, Van Dijck P.** 2015. Deletion of the DNA Ligase IV Gene in Candida glabrata
721 Significantly Increases Gene-Targeting Efficiency. Eukaryot Cell **14:**783-791.

Fig. 1 Mutant library screening reveals putative Cst6 kinase

S. cerevisiae wild type (WT) and mutants were grown in 5% CO_2 to exponential phase and either stayed at 5% CO_2 or transferred to air for 60 min. Sc*NCE103* expression was measured with qRT-PCR and normalized to WT expression under 5% CO_2 (for all data see supplemental table S2). ScSch9 was the most promising Cst6 kinase candidate. The bars show means ± standard deviation of ≥5 independent experiments. Significance against WT expression in the corresponding condition was calculated with two-sided t-test for unpaired samples and defined as * p≤0.05 and ** p≤0.01.

Fig. 2 Loss of ScSch9 enhances ScNce103 protein level and Sc*NCE103* promoter activation under 5% CO_2

(A) Endogenous ScNce103 levels of WT and mutants, cultivated in 5% CO_2 and air conditions, were detected by western blot analysis. *sch9*Δ showed elevated ScNce103 in 5% CO_2 compared to WT. Nce103 levels relative to the loading control and normalized to WT in 5% CO_2 are indicated below the blot.

(B) *S. cerevisiae* WT and mutants were transformed with GFP under control of Sc*NCE103* promoter and grown under 5% CO_2. Cells either stayed in this condition or were transferred to air for up to 120 min. Fluorescence was detected at time point of switch (0), after 60 min and 120 min. Quantification was done by measuring fluorescence intensity of at least 50 cells per time point. Significance of mutant against WT fluorescence at time point 0, calculated with two-sided t-test for unpaired samples, was defined as *** p≤0.001.

Fig. 3 ScSch9 interacts with and phosphorylates ScCst6

(A) ScCst6 was immunopurified from *S. cerevisiae* using specific antibodies and subsequently incubated with purified ScSch9-His. ScSch9 was only detectable when ScCst6 was previously bound.

(B) For *in vitro* phosphorylation assays, ScSch9-His was immunopurified from *S. cerevisiae* grown under 5% CO_2 and incubated with recombinant ScCst6-His in the presence of [γ-^{32}P] Adenosine 5'-triphosphate. Incorporation of γ-^{32}P was detected by autoradiography. A clear band for radioactively labeled ScCst6 was visible indicating phosphorylation of ScCst6 by ScSch9.

Fig. 4 ScCst6 phosphorylation at position S266 is crucial for Sc*NCE103* regulation

(A) ScCst6-His, overexpressed in WT under 5% CO_2, was affinity purified and subjected to SDS-PAGE. Corresponding bands were excised and digested with Trypsin-LysC, AspN, GluC or LysargiNase. Additionally, an in-solution digest for Trypsin-LysC and GluC was performed. Phosphorylated peptides were enriched and analyzed with LC-MS/MS. 19 different phosphorylation sites, indicated with P, were identified in at least 2 of 10 independent experiments**.** Newly identified phosphorylation sites are shown in bold, previously known sites are not bold. Underlined are the 3 serine residues that were conserved in *S. cerevisiae*, *C. glabrata* and *C. albicans*. Among them, only S266 was found to be phosphorylated in WT, marked with a border.

(B) Site-specific mutation of S266 was performed to investigate direct influence on Sc*NCE103* expression in changing CO_2 conditions. Expression levels were normalized to WT Sc*NCE103* expression in 5% CO_2. Changing S266 to alanine (*cst6*Δ + *CST6* ^{S266A}) showed a significant upregulation of Sc*NCE103* ^{CO2} while

Sc*NCE103* ^{air} levels were unaltered. This is comparable to expression changes of *sch9*Δ and proves the critical role of Cst6 S266 for CA regulation.

The bars show means ± standard deviation of 5 independent experiments. Significance against *cst6*Δ + *CST6*, calculated with two-sided t-test for unpaired samples, was defined as ** p≤0.01.

Fig. 5 *SCH9* function in CO_2 signaling is conserved in pathogenic yeasts

C. glabrata (A) and *C. albicans* strains (B) were grown under different CO_2 conditions and expression of *NCE103* was measured with qRT-PCR. Cg*NCE103* expression was normalized to control expression (AFG1), Ca*NCE103* expression to *C. albicans* WT, cultivated in 5% CO_2. Both species showed comparable regulation mechanisms. Deletion of *RCA1* led to significantly decreased *NCE103* ^{air} expression. *sch9*Δ mutants of *C. glabrata* and *C. albicans* increased *NCE103* ^{CO2} expression, consistent with findings for *S. cerevisiae*. This suggests a conserved role of *SCH9* in CO_2 signaling in all three yeast species.

The bars show means ± standard deviation of ≥4 independent experiments. Significance against control expression, calculated with two-sided t-test for unpaired samples, was defined as * p≤0.05, ** p≤0.01 and *** p≤0.001.

Fig. 6 Pkh1/2 but not TORC1 mediates activation of ScSch9 – ScCst6 signaling in 5% CO_2

(A) Phosphorylation of ScSch9 in 5% CO_2 was detected using LC-MS/MS. Phosphorylation of residues known to be addressed by ScPkh1/2 and TORC1 was detected.

(B) Sc*NCE103* ^{CO2} expression of WT and ScSch9 activator mutants was measured with qRT-PCR and normalized to WT expression. Single mutants of Sc*TOR1*, Sc*PKH1* or Sc*PKH2* did not change Sc*NCE103* ^{CO2} expression significantly. Furthermore, *S. cerevisiae* WT was treated with 200 nM rapamycin to inactivate TORC1 or DMSO as solvent control. Rapamycin treatment led to upregulation of Sc*NCE103* ^{CO2} expression, but it does not reach Sc*NCE103* ^{CO2} levels of *sch9*Δ. Because of Sc*PKH1/2* redundancy, a temperature sensitive double mutant in the background of 15 Dau was tested and revealed significantly increased Sc*NCE103* ^{CO2} levels. The bars show means ± standard deviation of ≥ 3 independent experiments. Significance against expression of WT + DMSO or 15 Dau, calculated with two-sided t-test for unpaired samples, was defined as * p≤0.05.

(C) Sc*NCE103* expression of *sch9*Δ + *SCH9* and revertants with *SCH9* possessing S/T to A mutations of known activation sites was measured in changing CO_2 and normalized to WT expression. Integration of *SCH9* in *sch9*Δ restored the WT regulation pattern of Sc*NCE103*. Phosphoablative mutation of the 6 phosphorylation sites known to be addressed by TORC1 (S711A, T723A, S726A, T737A, S758A, S765A), indicated as *SCH9* ^{6A}, showed no expression changes. Mutation of the *PKH1/2* site T570 increased Sc*NCE103* ^{CO2} expression significantly, indicating a reduced activation of ScSch9. Combination of mutations of phosphorylation sites addressed by both activators, *SCH9* $^{T570A, 6A}$, had no additional effect on Sc*NCE103* ^{CO2} expression, but Sc*NCE103* ^{air} expression was significantly enhanced. The bars show means ± standard deviation of ≥ 4 independent experiments. Significance against *sch9*Δ + *SCH9*, calculated with two-sided t-test for unpaired samples, was defined as * p≤0.05 and ** p≤0.01.

Fig. 7 Nce103 regulation model in changing CO_2 conditions

(A) In 5% CO_2 environment, Sch9 is activated by phosphorylation of T570 via Pkh1/2, whereby Pkh1/2 activity is influenced by phytosphingosine (PHS) and phosphatidylinositol (PI). Moreover, a direct influence of CO_2 levels on Sch9 activation is possible. Activated Sch9 phosphorylates the transcription factor Cst6, which is subsequently not able to induce *NCE103* expression. This results in very low Nce103 levels, which do not enhance CO_2 fixation.

(B) Under air conditions, Sch9 is not activated by Pkh1/2 and does not inhibit Cst6. Active Cst6 induces *NCE103* expression and enhances Nce103 protein level leading to fixation of CO_2. Furthermore, Nce103 seems to be induced by another, so far unknown mechanism.

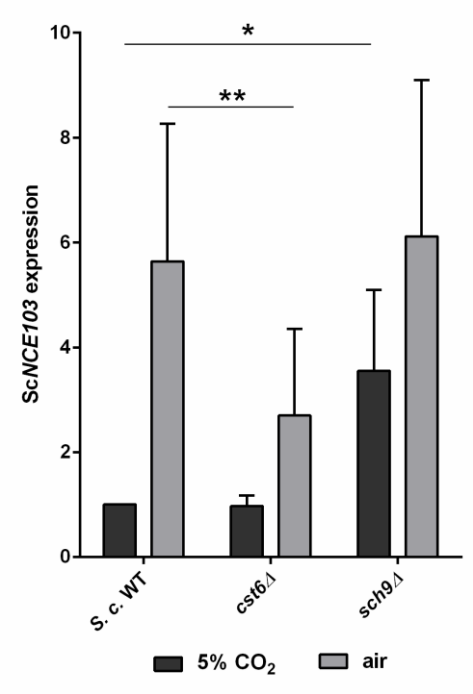

Fig. 1 Mutant library screening reveals putative Cst6 kinase

A

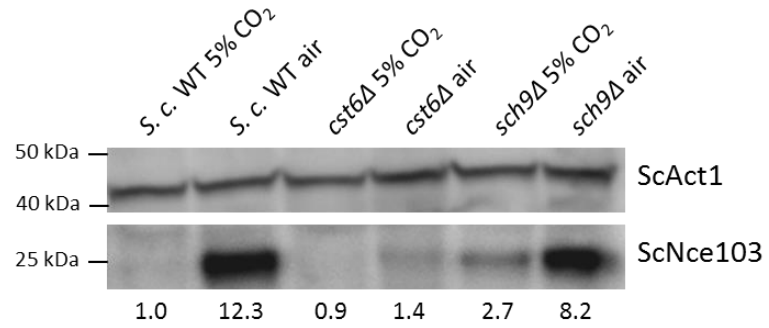

B

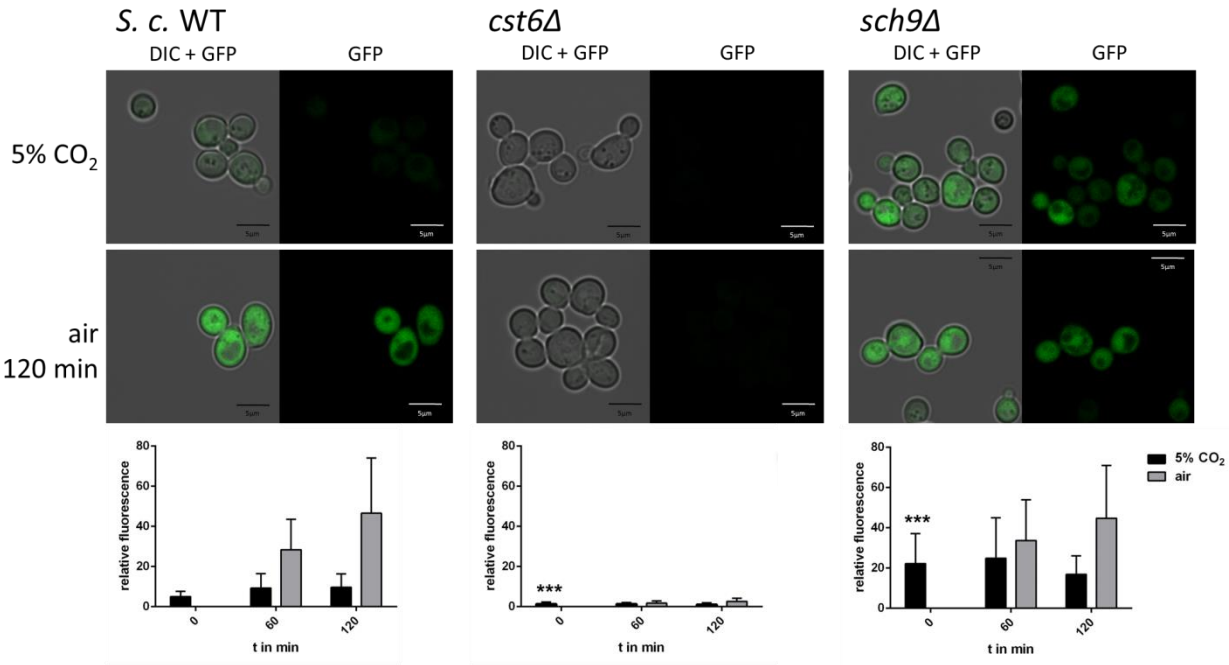

Fig. 2 Lack of ScSch9 enhances ScNce103 protein level and Sc*NCE103* promoter activation under 5% CO_2

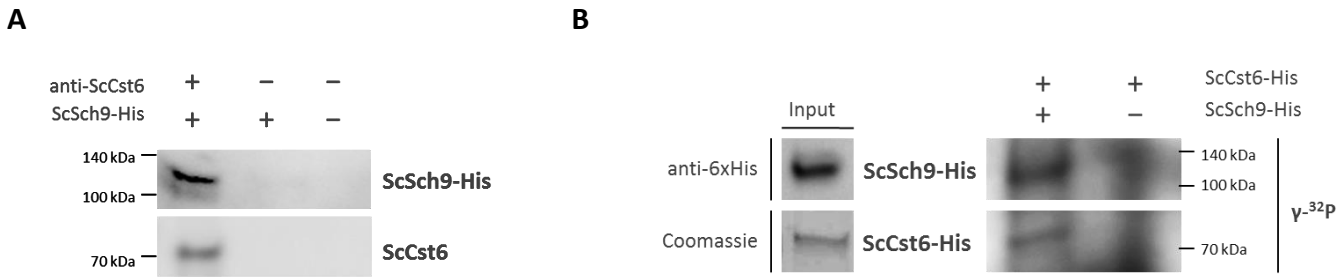

Fig. 3 ScSch9 interacts with and phosphorylates ScCst6

A

```
1    MFTGQEYHSV DSNSNKQKDN NKRGIDDTSK ILNNKIPHSV SDTSAAATTT STMNNSALSR SLDPTDINYS TNMAGVVDQI
                                                P

81   HDYTTSNRNS LTPQYSIAAG NVNSHDRVVK PSANSNYQQA AYLRQQQQQD QRQQSPSMKT EEESQLYGDI LMNSGVVQDM
           P  P                                                    P

161  HQNLATHTNL SQLSSTRKSA PNDSTTAPTN ASNIANTASV NKQMYFMNMN MNNNPHALND PSILETLSPF FQPFGVDVAH
                         P                    P

241  LPMTNPPIFQ SSLPGCDEPI RRRRISISNG QISQLGEDIE TLENLHNTQP PPMPNFHNYN GLSQTRNVSN KPVFNQAVPV
                               P                                          P

321  SSIPQYNAKK VINPTKDSAL GDQSVIYSKS QQRNFVNAPS KNTPAESISD LEGMTTFAPT TGGENRGKSA LRESHSNPSF
                              P                    P                          P P

401  TPKSQGSHLN LAANTQGNPI PGTTAWKRAR LLERNRIAAS KCRQRKKVAQ LQLQKEFNEI KDENRILLKK LNYYEKLISK
P      P

481  FKKFSKIHLR EHEKLNKDSD NNVNGTNSSN KNESMTVDSL KIIEELLMID SDVTEVDKDT GKIIAIKHEP YSQRFGSDTD
                                                                          P     P P

561  DDDIDLKPVE GGKDPDNQSL PNSEKIK
                         P    P
```

B

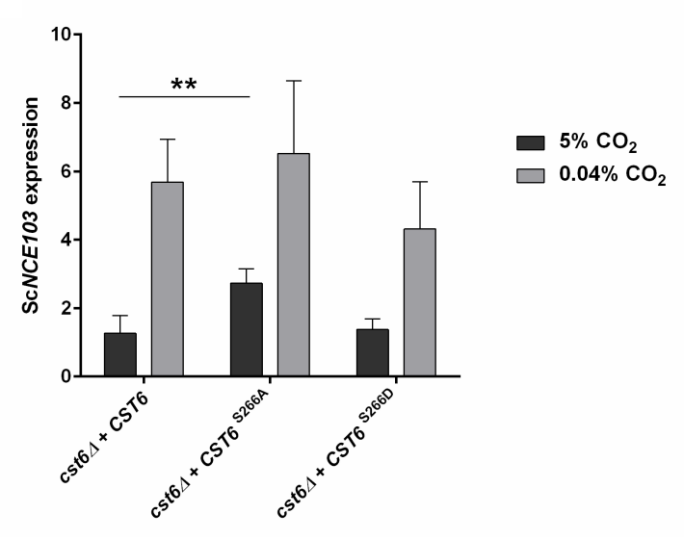

Fig. 4 ScCst6 phosphorylation at position S266 is crucial for Sc*NCE103* regulation

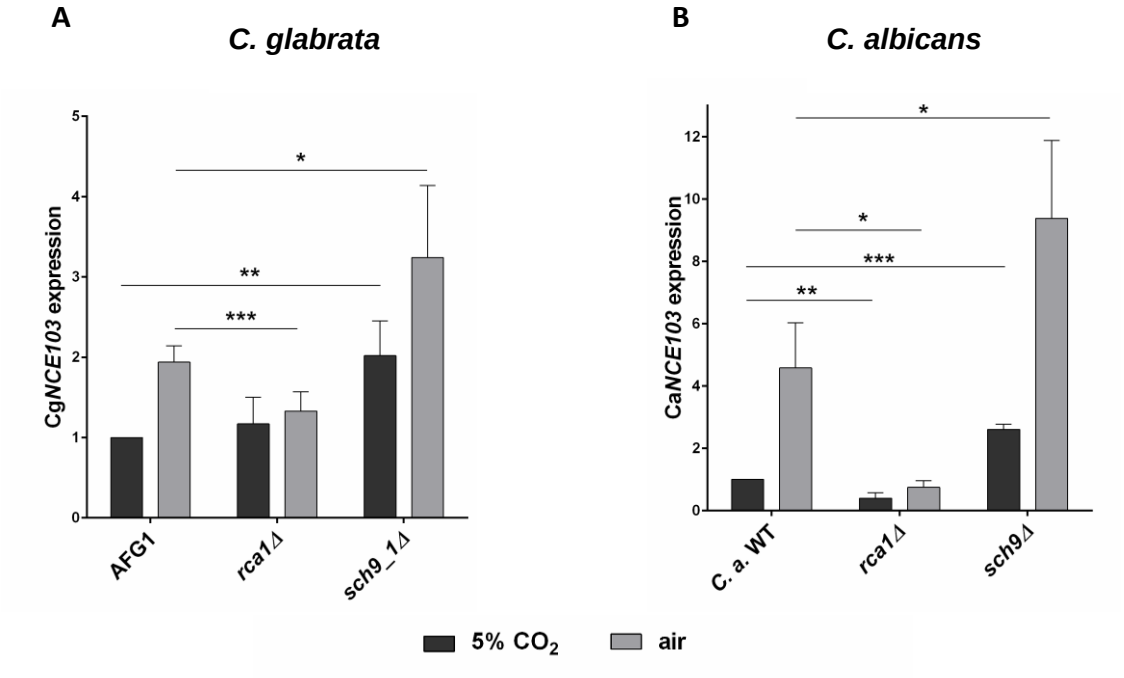

Fig. 5 *SCH9* function in CO_2 signaling is conserved in pathogenic yeasts

A

Phosphorylation by	Phosphorylated in 5% CO_2
ScPkh1/2	T570
TORC1	S726
	S758
	S765

B

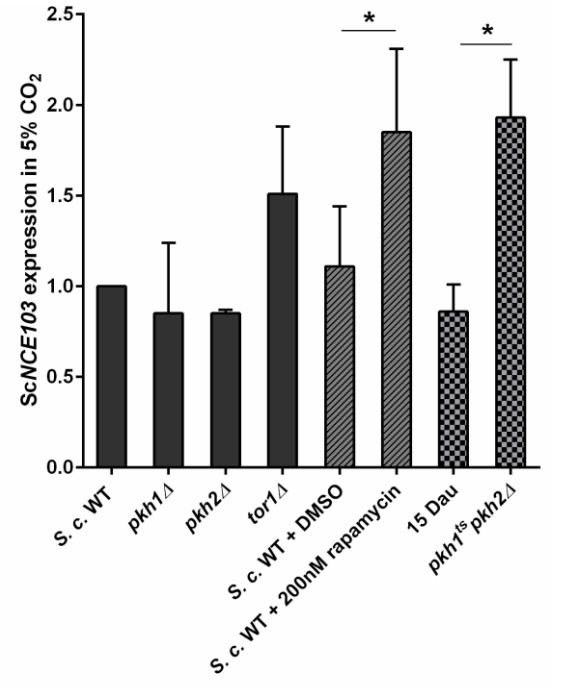

C

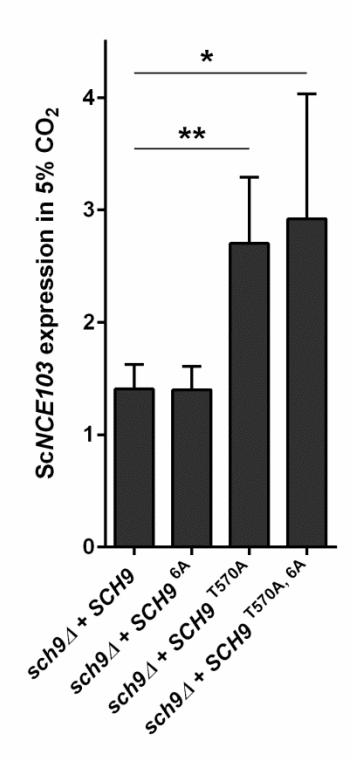

Fig. 6 Pkh1/2 but not TORC1 mediates CO_2-dependent activation of ScSch9 – ScCst6 signaling

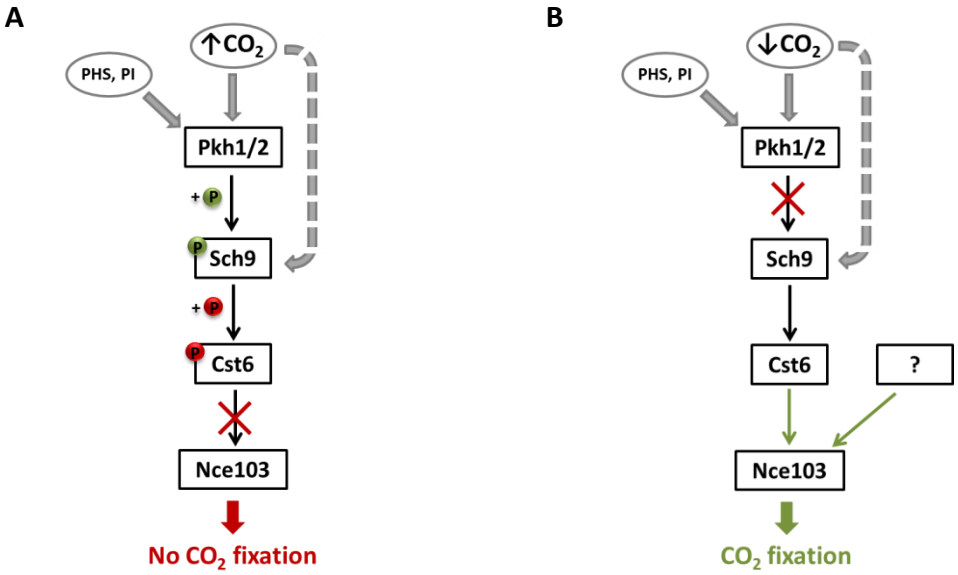

Fig. 7 Nce103 regulation model in changing CO_2 conditions